ENVIRONMENTAL ENGINEERING SCIENCE
Volume 39, Number 3, 2022

DOI: 10.1089/ees.2020.0374

Product Characterization of Hydrothermal Liquefaction and Supercritical Water Gasification of Water Hyacinth

Zeqin Liao,[1] Cen Wang,[2] Xingying Tang,[1,*] Yinghui Wang,[1] Zitao Lin,[1] Pengwei Ren,[1] Lihang Wang,[1] Haidong Xu,[3] Jianqiao Yang,[3] and Jianjun Cai[4]

[1]*Guangxi Key Laboratory on the Study of Coral Reefs in the South China Sea, School of Marine Sciences, Guangxi University, Nanning, China.*
[2]*Shaanxi Province Institute of Water Resources and Electric Power Investigation and Design, Xi'an, China.*
[3]*Key Laboratory of Thermo-Fluid Science and Engineering of MOE, School of Energy and Power Engineering, Xi'an Jiaotong University, Xi'an, China.*
[4]*Department of Building Environment and Energy Application Engineering, School of Architecture and Traffic, Guilin University of Electronic Technology, Guilin, China.*

Received: September 13, 2020 *Accepted in revised form: July 21, 2021*

Abstract

Hydrothermal liquefaction (HTL) and supercritical water gasification (SCWG) are promising technologies for clean renewable energy production from biomass. This study investigated the process and mechanism of water hyacinth treatment by HTL and SCWG to prepare clean biodiesel and combustible gas. The optimal HTL reaction conditions were 350°C, 50 min, 20 wt % stock concentration, and 0.60 g/mL water density. The liquid products were analyzed by Gas chromatograph-mass spectrometer and infrared radiation spectra analysis. The fat was hydrolyzed into fatty acids and the fatty acid decarboxylate formed alkanes. The protein undergoes C-N peptide bond hydrolysis and Maillard reaction with aldose to form ketones and nitrogenous compounds. The polysaccharides were hydrolyzed and cycled to form phenols. The optimal SCWG reaction conditions were 480°C, 20 min, 23.10% stock concentration, and a pressure between 25 and 27 MPa. The effects of process parameters on the content of H_2 and CH_4 in the gas products were studied. This work is helpful for resource utilization of water hyacinth hydrothermal treatment. The energy conversion efficiency of SCWG of water hyacinth in this experiment is lower compared with HTL.

Keywords: gasification; hydrothermal liquefaction; resource utilization; water hyacinth

Introduction

Water hyacinth is a common aquatic organism, which has vigorous vitality and rapid growth and reproduction, which has caused serious social and environmental problems. For the resource utilization of water hyacinth, hydrothermal liquefication (HTL) to produce biodiesel and supercritical gasification to produce hydrogen were considered, which not only meet the demand for renewable new energy and relieve energy pressure to a certain extent but also deal with environmental problems caused by excessive reproduction of water hyacinth (Mishima *et al.*, 2008; Yeh *et al.*, 2012; Toor *et al.*, 2011).

HTL is an important method to convert biomass into biodiesel. HTL refers to the process in which biomass is hydrolyzed to produce bio-oil under the conditions of subcritical temperature (about 300°C) and maintaining water at a liquid state (Kunaver *et al.*, 2010). In the process of HTL, the material did not need a drying process, indicating the energy consumption reduction and the cost saving (Elliott *et al.*, 2015). In addition, the fat, protein, and polysaccharide components could be changed to high-calorific bio-oil by HTL (Faeth *et al.*, 2013). HTL could also facilitate the separation, recovery, and reuse of nutrients in the process, such as nitrogen, phosphorus, iron, calcium, magnesium, potassium, and other mineral elements, as well as polar organic compounds (Duan and Savage, 2010; Dimitriadis and Bezergianni, 2017).

The supercritical water gasification (SCWG) technology has a good effect on the treatment of organic matter and biomass (Peterson *et al.*, 2008). Compared with the conventional gasification of biomass, the SCWG of biomass had

**Corresponding author:* Guangxi Key Laboratory on the Study of Coral Reefs in the South China Sea, School of Marine Sciences, Guangxi University, No. 100 East Daxue Road, Xixiangtang District, Nanning 530004, Guangxi Autonomous Region, China. *Phone:* +07713237721; *Fax:* 0771-3227855; *E-mail:* tangxingying@gxu.edu.cn

the following characteristics: the biomass depolymerization rate was very fast, reducing the content of coke; gasification had a better effect, the biomass gas rate could reach or even exceed 100%, and the percentage of H_2 in the gas product can even exceed 50% (Reddy *et al.*, 2014; Rodriguez Correa and Kruse, 2017). Many studies have been conducted on the gasification of biomass and corresponding model compounds in supercritical water to produce hydrogen (Demirbaş, 1998; Minowa and Inoue, 1999; Kruse and Gawlik, 2003; Nanda *et al.*, 2018).

In previous studies, little work has been done on the resource utilization of water hyacinth. In this article, the research directions meet the needs of national development of renewable biodiesel and turn water hyacinth into energy, which has great research value and practical value. According to the HTL experimental conditions of other biomass, the reaction conditions of HTL and SCWG of water hyacinth were explored and the reaction parameters were optimized to get the best oil yield quality and the highest hydrogen yield efficiency. In the process, the reaction mechanism of the liquefaction and gasification process was compared to provide theoretical basis and technical support for the resource utilization of water hyacinth, which would help to promote industrial application of HTL and SCWG.

Materials and Methods

Materials

The raw materials used in the experiment were water hyacinth salvaged from the Qin Jiang River in Qinzhou, near Beibu Gulf in the south of China. The volume of the reaction kettle used in this experiment was 2.7 mL (HTL) and 4.0 mL (SCWG). The shredding and cleaning were the necessary pretreatment for the quantitative research of water hyacinth. After drying at 50°C, the water hyacinth was crushed into powder by a small pulverizer and screened through a 100-mesh sieve. The dry water hyacinth powder with a particle size of 150 μm would be used as experimental material.

Elemental analysis of water hyacinth. The water hyacinth powder was measured by 50 mg, and the elements of C, H, O, N, P, and S in the water hyacinth powder were quantitatively analyzed by an elemental analyzer. The water and ash content in the samples were also tested. The analysis results of water hyacinth powder elements are shown in Table 1.

Among them, C_d is dry base carbon, H_d is dry base hydrogen, O_d is dry base oxygen, N_d is dry base nitrogen, P_d is dry base phosphorus, and $S_{t,\,d}$ is dry base total sulfur.

Analysis of the chemical composition of water hyacinth. The main chemical components of water hyacinth were protein, lipid, and polysaccharide. Protein content was determined by the determination of protein in foods (GB 5009.5-2010 of China). The protein in water hyacinth was decomposed under the heating condition of copper sulfate, potassium sulfate, and sulfuric acid, and the resulting ammonia reacted with sulfuric acid to form ammonium sulfate. After alkaline distillation of ammonium sulfate, free ammonia was generated and absorbed by boric acid. Then it was titrated with hydrochloric acid standard solution to calculate the protein content in water hyacinth.

The lipids in water hyacinth mainly refer to the fat inside the cell. Soxhlet extraction method was adopted in the determination of lipid content, and petroleum ether was the fat-soluble solvent used.

Anthracene colorimetric method was used for the determination of polysaccharides. Furfural or its derivatives were formed by dehydration of saccharides and condensation of anthracene at a higher temperature to form a blue complex. The absorption peak appeared at 620 nm and was calculated by comparing it with the standard curve. The chemical composition of water hyacinth is shown in Table 2.

Apparatus and procedures

The micro-batch reactor used in the experiment was assembled by Swagelok serial port connection and 1/2′ to 1/8′ of dissimilar joint. The outlet was connected to a 9′ long 1/8 outside diameter stainless steel tube and a 30,000 psi high-pressure valve. Techne SBL-2D sand bath was used to heat the miniature reactor, and Techne TC-8D control instrument was used to control the temperature. The reactor was placed vertically in a metal basket and the main body was immersed in the sand bath to ensure adequate heat transfer.

According to the targeted reaction temperature and pressure, the corresponding water density was calculated by the water vapor property software (WaterPro) to obtain the amount of feed and water quantity needed for the reaction. The temperature was heated up to the required temperature of the experiment, and the reactor was put into the sand bath after the reactor temperature was stable at the set temperature. When the set reaction time was reached, the reactor was taken out and cooled by cool water. After the feed was taken out and left to stratify, the centrifuge tube was put into a centrifuge for centrifugation. Then vacuum distillation was carried out, and the water phase was analyzed.

A 50-mL spherical flask was used in vacuum distillation, and its weight (M) was recorded. Then the organic phase was poured into a flask, and a rotary evaporator was used to remove dichloromethane in the organic phase. The spherical flask was taken down, the outer wall was cleaned with absolute ethanol, the flask was dried with a blower, and the weight (M1) was recorded. To calculate the total oil output (X), the weight of the previous flask was subtracted from the weight at this time (Shakya *et al.*, 2017) [Eq. (1)].

Table 1. Element Analysis of Water Hyacinth Powder

C_d/wt %	H_d/wt %	O_d/wt %	N_d/wt %	P_d/wt %	$S_{t,\,d}$/wt %	Moisture/wt %	Ash/wt %
37.93	5.60	37.00	4.28	0.10	1.34	5.62	8.13

C_d, dry base carbon; H_d, dry base hydrogen; N_d, dry base nitrogen; O_d, dry base oxygen; P_d, dry base phosphorus; $S_{t,\,d}$, dry base total sulfur.

Table 2. Chemical Composition of Water Hyacinth

Protein/wt %	*Lipids/wt %*	*Polysaccharides/wt %*
21.41	3.57	64.79

$$X = M1 - M \quad (1)$$

A certain amount of n-hexane was added into the spherical flask and the flask was shaken for mixing. The insoluble was heavy bio-oil. The rotary evaporator was used to remove the residual n-hexane in the flask. The flask was taken off, and the outer wall was cleaned with absolute ethanol. The flask was blown dry, weighed, and recorded (M2). The weight of the empty flask was subtracted to obtain the heavy bio-oil production (Y).

The experimental flow of SCWG and HTL of water hyacinth was roughly the same, but there were some differences. In the experimental flow of SCWG, the reactor was filled with helium gas as an internal standard and the reactor was connected to the gas chromatography for gas composition analysis. The other experiment flow of SCWG was the same as HTL.

Analysis

The total carbon content (TC) in the aqueous phase products was measured by a total organic carbon analyzer (ET1020A). The quality of the water hyacinth sample and the items to be weighed in the experiment were weighed by an electronic scale (XA105). The gas composition and the percentage of the product of supercritical gasification reaction were analyzed by a gas chromatography analyzer (3420A). The organic compounds in the oil phase after HTL were analyzed by a gas chromatograph-mass spectrometer (GC-MS) (GC6890 and MS5973). The oil phase products after HTL were analyzed by an infrared spectrometer (Nexus 470). Elements in bio-oil were analyzed by an elemental analyzer (Vario ELIII).

Results and Discussion

Experimental study on the production of bio-oil by hydrothermal liquefaction of water hyacinth

The influence of reaction conditions on the oil yield of hydrothermal liquefaction of water hyacinth. Figure 1 shows an influence curve of reaction temperature, reaction time, feed concentration, and water density on total oil yield and heavy oil yield.

Influence of reaction temperature. The reaction time was set as 20 min, the material concentration was 9.09%, and the reaction pressure was maintained at 18 MPa. Figure 1a shows the influence of reaction temperature on the hydrothermal liquefaction oil yield of water hyacinth. The oil yield was equal to mass of oil over initial mass of feedstock.

As shown in Fig. 1a, the temperature had a decisive influence on the HTL oil yield of water hyacinth. The oil yield of HTL of water hyacinth first increased and then decreased with increasing reaction temperature, and the influence curve showed a parabolic shape.

At 350–390°C, the oil production rate gradually decreased from the highest value to 14.35%, indicating that at a higher reaction temperature, the fatty acid content of bio-oil decreased due to further pyrolysis of bio-oil. The influence trend of temperature on the total oil yield and the heavy oil yield curve was the same.

At 200°C, the HTL rate of water hyacinth was very low, only 3.21%, and hardly any liquefaction reaction occurred. Near the critical point (374°C, 22.1 MPa), the ionic product of water increased sharply. Under this condition, high H^+ and OH^- concentrations could have a specific catalytic effect on the ionic hydrolytic reactions of many complex carbon-containing compounds (Bo *et al.*, 2018).

Under such conditions, sugar, protein, and fat macromolecules were prone to isomerization, recombination, depolymerization, and condensation reactions, and catalyzed the generation and intensification of the decarboxylation reaction, pyrolysis, water vapor reforming, and gasification reactions of

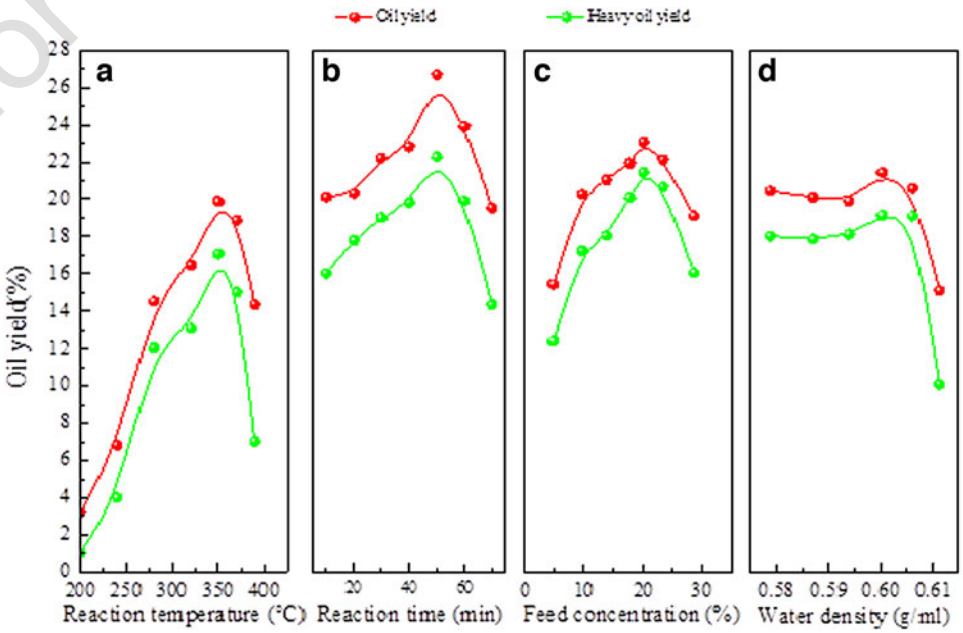

FIG. 1. Influence curve of reaction temperature **(a)**, reaction time **(b)**, feed concentration **(c)**, and water density **(d)** on total oil yield and heavy oil yield. **(b–d)** At 350°C.

the intermediate products, eventually leading to a higher production of gas products and a lower production of bio-oil.

According to the above analysis, the reaction temperature significantly influenced the oil yield of HTL of water hyacinth. The influence of different temperature ranges on the HTL of water hyacinth was determined. Among them, the hydrolysis of large molecular compounds in water hyacinth was dominant below 220°C, and at this time, most small molecular organic compounds after hydrolysis were dissolved in water.

Therefore, the oil production rate of HTL of water hyacinth at 200°C was only 3.21%. With increasing temperature, the polymerization, condensation, and hydrolysis reactions formed a competitive situation in the process of HTL in the range of 240–320°C. The oil yield of water hyacinth increased rapidly, from 6.82% to 16.47%, which indicated that some small organic matter was converted into bio-oil, leading to a higher bio-oil yield (Amrullah and Matsumura, 2017).

The oil yield reached the maximum value at 350°C, and then the concentration of water-soluble organics gradually decreased. Pyrolysis and gasification reactions dominated after exceeding the critical temperature, so the temperature range suitable for HTL of water hyacinth was 320–370°C.

Influence of reaction time. An appropriate reaction time makes the process of hydrothermal liquefaction of water hyacinth more economical and effectively reduces equipment costs and operating costs (Uddin *et al.*, 2014; Duan *et al.*, 2018). This experiment studied the effect of reaction time on the hydrothermal liquefaction oil yield of water hyacinth at 350°C, a material concentration of 9.09%, and water density of 0.5869 g/mL.

Figure 1b shows the influence of different reaction times on the yield of bio-oil. As shown in the figure, the bio-oil yield of water hyacinth hydrothermal liquefaction first increased and then decreased with increasing reaction time. There was an appropriate reaction time range for water hyacinth HTL. In the range, the longer the reaction time was, the higher the bio-oil yield would be. In the first 10–50 min, the oil production rate increased with increasing time at 350°C, reaching a maximum value of 26.70%.

However, the oil production rate was reduced after 50 min because water hyacinth would be hydrolyzed and depolymerized to small-molecule compounds at the beginning of the reaction. The reaction time was prolonged, and these small molecules recombined to form bio-oil by condensation or repolymerization. However, if the response time of the best values continued to extend the time, a large amount of coke was produced due to cyclic formation and condensation of bio-oil components and some of the products with lower molecular weights would be gasified by pyrolysis to produce many gases or small molecules of water-soluble compounds transferred to the gas phase (Valdez *et al.*, 2012).

Influence of feed concentration. As a feed, the appropriate concentration can significantly improve the oil yield, oil quality, and economy. Under the conditions of a reaction temperature of 350°C, a reaction time of 20 min, and a water density of 0.5869 g/mL, the influence curve of water hyacinth's hydrothermal liquefaction oil yield was obtained by changing the material concentration, as shown in Fig. 1c.

The total yield of bio-oil and heavy oil increased slowly as the feed concentration increased from 4.76 to 20 wt % and reached the highest value of 23.07% at 20 wt %. The material concentration continued to increase, and the yield of oil decreased. The oil yield at a feed concentration of 28.57 wt % was similar to the total oil yield of 19.09%, and the yield of heavy oil was lower. With increasing feed concentration, the concentration of activated molecules in the reactants increased, and the probability of effective collision between molecules increased under high-temperature and high-pressure conditions. According to Le Chatelier's principle, when the reaction rate of the product was constant, the reaction moved in the direction of a positive reaction, so the oil yield increased.

However, in the case of a high reaction rate, the concentration of reactants continued to increase, and oil production would not increase simultaneously.

Moreover, intermediate products were more likely to undergo a series of complex reactions, such as polycondensation, polymerization, and cyclization, to form tar and carbon deposition, which would lead to a decrease in the oil yield accordingly. Although a lower material concentration could effectively improve the oil production rate and bio-oil quality, a higher water content required higher energy consumption, which was uneconomical for the whole treatment process, and the subsequent sewage treatment was costly.

Influence of water density. In HTL, the water density was directly reflected by the reaction pressure. With increasing reaction temperature, especially above the critical temperature, the pyrolysis reaction, and the formation of more gas products are liable to occur. However, increasing the water density was more conducive to the hydrolysis reaction because increasing the water density could be conducive to increasing the H^+ released by water at high temperature, thus increasing the effect of the acid-catalyzed reaction. Therefore, the influence of water density on the HTL of water hyacinth was analyzed. As shown in Fig. 1d, the water density ranged from 0.5787 to 0.6112 g/mL under 350°C, 20 min, and a 9.09 wt % feed concentration.

As shown in Fig. 1d, the water density has little effect on the HTL of water hyacinth. The total yield of bio-oil was $\sim$20.5%, and the yield of heavy oil was $\sim$18%, which shows that a higher density of water is not better. In contrast, the higher the water density was, the higher the pressure required at the same temperature. This increased the equipment pressure resistance condition requirement and was not conducive to reducing the operation cost of the whole system of HTL of water hyacinth.

However, the total oil production rate and heavy oil yield of water hyacinth decreased at a water density of 0.6112 g/mL. This was because the corresponding reaction pressure was 22 MPa and the reaction temperature was 350°C. In the near-critical region, the ionic product and dielectric constant of water change significantly, which is conducive to the gasification reaction, and the gas phase products increase, so the oil production rate decreases (Peterson *et al.*, 2008).

The optimal reaction conditions of hydrothermal liquefaction of water hyacinth were 350°C, 50 min, feed concentration of 20 wt %, and water density of 0.6002 g/mL.

The influence of reaction conditions on the migration and transformation of carbon during hydrothermal lique

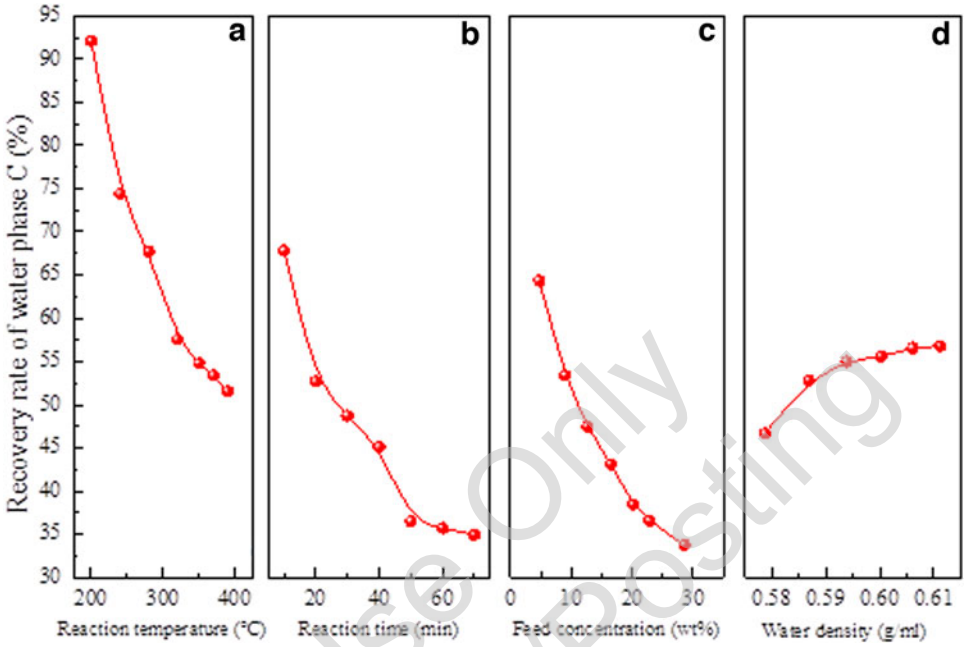

FIG. 2. Effect of reaction temperature **(a)**, reaction time **(b)**, feed concentration **(c)**, and water density **(d)** on the recovery of aqueous Phase C. **(b–d)** At 350°C.

faction. Figure 2 shows an effect of reaction temperature, reaction time, feed concentration, and water density on the recovery of aqueous Phase C.

Influence of reaction temperature. Figure 2a shows the effect of reaction temperature on the recovery of carbon in the aqueous phase. The experimental conditions were 20 min, 9.09 wt % feed concentration, and 18 MPa water density. The recovery of carbon in the aqueous phase decreased with increasing temperature, and in the low-temperature range, the recovery of carbon in the aqueous phase decreased significantly with increasing temperature.

In contrast, the recovery of carbon in the aqueous phase decreased gently in the range of 320–390°C. These results indicated that the macromolecular organic matter in water hyacinth was first hydrolyzed and dissolved in the water phase, leading to the high carbon content in the water phase (Toor *et al.*, 2011). The temperature was a key factor affecting the oil production rate of water hyacinth. At low temperatures, these small molecular organic compounds did not easily polymerize and recombine to form bio-oil.

With increasing temperature, the active molecular content increased, the probability of effective collision increased, the oil production rate increased gradually, and carbon gradually migrated to the bio-oil. Then, with the reaction temperature continuing to increase, although the bio-oil production declined, it was more conducive to the gasification reaction, and carbon was transferred to the gas-phase product. As a result of the comprehensive action, the recovery rate of aqueous phase C decreased slowly.

Influence of reaction time. Figure 2b shows the effect of reaction time on the carbon recovery rate of hydrothermal liquid aqueous phase products at a constant temperature of 350°C, a material concentration of 9.09%, and water density of 0.5869 g/mL. The recovery rate of C in the aqueous phase decreased with increasing time. Within the time interval of 10–50 min, the recovery rate of carbon in the aqueous phase decreased significantly with time, from 62.79% at 10 min to 36.52% at 50 min.

A prolonged reaction time was conducive to the progress of the oil production reaction and the increase in the oil production rate. After 50 min of reaction, the C recovery rate in the aqueous phase decreased slowly and tended to be stable, indicating that the polymerization and recombination of small molecules were sufficient and that the reaction reached equilibrium. The decrease of the C recovery rate in water indicated that the amount of carbon transferred to water was reduced after HTL of the water hyacinth material, suggesting the amount of water-soluble organic matter was reduced and carbon transferred to the bio-oil or the gas phase.

Influence of feed concentration. Figure 2c shows the carbon recovery trend in the water phase of different water hyacinth feed concentrations under the reaction temperature of 350°C and water density of 0.5869 g/mL for 20 min. There was a negative correlation between the carbon recovery rate in the aqueous phase and the water hyacinth material concentration, which decreased from 64.3% when the concentration of material was 4.76 wt % to 33.74% when the feed concentration was 28.57 wt %.

In other words, with increasing material concentration, the concentration of activated molecules increased, which was conducive to the reaction toward the direction of oil production, and the transfer of carbon to bio-oil increased. The more water hyacinth was added, the lower mobility of the carbon from the raw material into the aqueous phase. As the feed concentration exceeded 20 wt %, the oil yield decreased and the water phase C recovery continued to fall because the intermediate hydrolysis products were liable to condense and change into macromolecular compounds as tar. Therefore, the water recovery rate of C would continue to decrease with increasing feed concentration.

Influence of water density. Figure 2d shows the influence of water density changes on C recovery in the aqueous phase under the reaction conditions of 350°C, reaction time 20 min, and material concentration of 9.09%. With increasing water density, the mobility of carbon in the raw material to the aqueous phase increased slowly from 46.68% to 56.8%. As the water density increased, the pressure in the reactor increased. At the same time, the oil yield did not change significantly, and the C recovery rate in the water phase increased slowly, indicating that the increased water density promoted the hydrolysis of organic matter that was more difficult to dissolve in water.

The above results showed that temperature, time, material concentration, and water density, all had an impact on the migration and transformation of carbon, among which temperature, time, and material concentration had significant impacts. With increasing temperature, time, and material concentration, the recovery rate of aqueous phase carbon decreased significantly, and the reduction rate gradually slowed down. As the water density increased, the recovery rate of the water phase carbon increased slowly.

The influence of reaction conditions on the migration and transformation of nitrogen in hydrothermal liquefaction. Figure 3 shows an effect of reaction temperature, reaction time, feed concentration, and water density on the recovery of aqueous Phase N.

Influence of reaction temperature. The reaction time, the material concentration of 9.09 wt % and the reactor's pressure remained unchanged at 18 MPa. Figure 3a displays the relationship between the content of nitrogen in the aqueous phase and the reaction temperature.

As seen from the figure, with increasing hydrothermal liquefaction temperature of the water hyacinth, the proportion of nitrogen in the water hyacinth migrating to the water phase increased continuously, and the change was approximately linear. At 200°C, the recovery rate of nitrogen in the aqueous phase was 5.29%, while at 390°C, the recovery rate of nitrogen in the aqueous phase increased to 48.37%. Nearly half of the nitrogen in the raw materials migrated into the aqueous phase. This result suggested that as the temperature increased, proteins were converted into bio-oil, and small water-soluble molecules were produced.

In the process of HTL of biomass, nitrogen would hardly be converted into gas phase product N_2 and migrate to liquid phase product (Valdez *et al.*, 2012). The nitrogen content in water hyacinth was 4.28 wt % and water hyacinth likely enriched the nitrogen in the eutrophication water body. Therefore, biodiesel production from water hyacinth as a raw material could control the eutrophication pollution of lakes and reservoir water quality. The content of ammonia, nitrogen, and organic matter in the water phase after HTL was higher than the emission standard; therefore, follow-up water treatment was needed.

Influence of reaction time. Figure 3b shows the relationship between the N recovery rate and reaction time in the aqueous phase. The reaction temperature of 350°C, the material concentration of 9.09 wt %, and the water density of 0.5869 g/mL were left unchanged. As seen from the figure, the nitrogen recovery in the aqueous phase product of water hyacinth after HTL showed a rising trend with increasing time, and the nitrogen recovery increased from 32.04% of the reaction time of 10 min to 42.15% of the reaction time of 70 min. Overall, the change range of nitrogen recovery in the

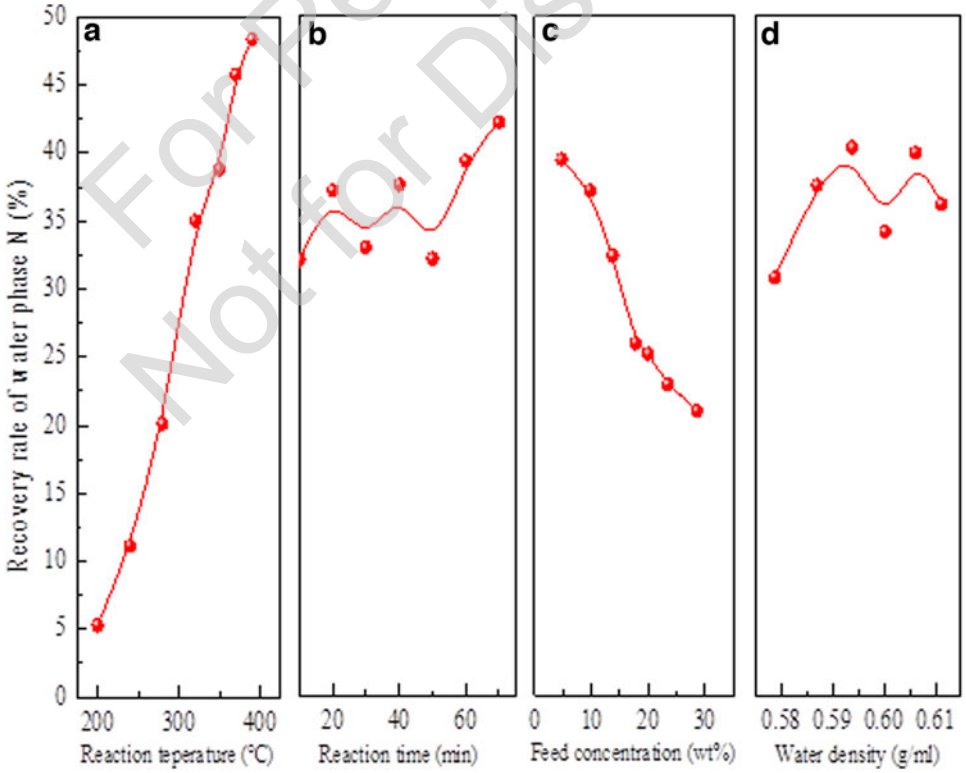

FIG. 3. Effect of reaction temperature **(a)**, reaction time **(b)**, feed concentration **(c)**, and water density **(d)** on the recovery of aqueous Phase N. **(b–d)** At 350°C.

water phase with time was not great, indicating that reaction time was not the main parameter that restricted protein molecular hydrolysis and bond breaking.

Influence of feed concentration. Under the conditions of 350°C, 20 min, and 0.5869 g/mL, the effect of feed concentration on the recovery rate of nitrogen in water phase products of HTL of water hyacinth is shown in Fig. 3c. The changing trend of nitrogen recovery in the aqueous phase was evident. With increasing feed concentration, N recovery decreased from 39.41% of the feed concentration of 4.76 wt % to 20.96% of the feed concentration of 28.57 wt %. This result showed that high-temperature and high-pressure water as a reactant participated in water hyacinth hydrothermal liquefaction. As the water hyacinth concentration increased, the amount of water corresponding to the material per unit mass decreased. The unreacted HTL of proteins resulted in most nitrogen remaining in the oil phase products and high nitrogen content in the bio-oil.

Influence of water density. In HTL, ionized H^+ and OH^- ions contributed to the chain breaking and hydrolysis of long-chain protein macromolecules. The reaction temperature was determined to be 350°C, the reaction time was determined to be 20 min, the material concentration was determined to be 9.09 wt %, and the water density was changed. The relationship between the recovery rate of nitrogen in the water phase product after HTL of water hyacinth and the water density is shown in Fig. 3d. The lowest N recovery was 30.73% under a water density of 0.5787 g/mL, and the highest nitrogen recovery was 40.30% under a water density of 0.5938 g/mL. The recovery of nitrogen in the aqueous phase product was almost independent of the water density.

Mechanism of hydrothermal liquefaction of water hyacinth

Analysis of hydrothermal liquid oil phase products of water hyacinth

GC-MS analysis. The hydrothermal liquefaction experiment of water hyacinth was carried out on a batch reactor under the experimental conditions of 350°C, 20 min, 9.09 wt %, and 0.5787 g/mL. After the end of the experiment, pure CH_2Cl_2 was used to extract the organic matter from the liquid products by liquid chromatography. A representative bio-oil was selected, and the composition of organic matter was qualitatively analyzed by GC-MS. Table 3 shows the organic matter composition corresponding to each obvious peak value. The bio-oil obtained from hydrothermal liquefaction of water hyacinth had a wide variety of organic compounds, nearly 100, of which 42 are listed in Table 3. These compounds accounted for 78% of the peak area.

As shown in Table 3, the bio-oil contained a variety of long-chain alkanes and their derivatives. The peak area ratio of C_9–C_{28} compounds, such as dodecane and n-pentadecane, reached 21.16%. There were also some free fatty acids, such as pentadecanoic acid, palmitic acid, and octadecanoic acid, in addition to long-chain alkanes. These long-chain alkanes and fatty acids directly led to the high viscosity of the bio-oil and seriously affected its transport performance. Free fatty acids are a direct product of triglyceride hydrolysis in fats. Some studies have found that free fatty acids are chemically stable in subcritical water.

However, as the temperature rose to 310°C, long-chain fatty acids generated aliphatic hydrocarbons through decarboxylation reactions, which made the amounts of long-chain alkanes in bio-oil higher than those of fatty acids. With the temperature rising further to the critical temperature point, the unstable fatty acid decomposition products became more complex and even led to the decomposition of long-chain alkanes into gas products such as CO_2, CO, and H_2.

In addition to long-chain alkanes and fatty acids, bio-oil also contained a certain amount of phenols and their derivatives, and aromatic compounds and their derivatives. The main chemical component of water hyacinth was cellulose, which produced phenols and their derivatives through depolymerization in HTL.

Water hyacinth is rich in chlorophyll, which contains a pyrrole ring monomer. Chlorophyll hydrolyzes and forms indoles. Indoles have a C-N bond in their molecular structure and are very stable under hydrothermal conditions. The C-N bond is electron bonding, low in energy, and stable in nature, making nitrogen removal difficult. Compounds containing nitrogen are also amides and amines, such as hexadecanoamide and succinimide, but the content is relatively small. The nitrogenous substances were produced by the condensation or repolymerization of amino polymers following the breakdown of protein–peptide bonds during the hydrothermal reaction.

Another important class of organic compounds was ketones, which were intermediates of a series of complex Maillard reactions in the hydrothermal liquefaction of water hyacinth after the hydrolysis of polysaccharides and amino acids from protein hydrolysis. Heteroatom O in bio-oil mainly existed in free fatty acids and ketones. With increasing reaction temperature and reaction time, the free fatty acids would be decarboxylated to their corresponding long-chain alkane, the ketones would be dehydrogenated to form reducing ketones or aldehydes, and the oxygen content in bio-oil would decrease.

Infrared spectrum analysis. According to the qualitative analysis of bio-oil GC-MS, the main oil phase products from water hyacinth hydrothermal liquefaction were mainly single aromatic compounds and their derivatives, such as benzene, toluene, and phenol; aliphatic compounds and their derivatives, such as n-pentadecane, n-hexadecane, and 2-methyl hexadecane; oxy compounds, such as ketones such as long-chain carboxylic palmitate, 2-hexadecane; nitrogenous compounds, such as amines, amides, indole, etc.; polycyclic aromatic hydrocarbons and their derivatives, such as naphthalene.

To verify the composition of water hyacinth hydrothermal liquid bio-oil, the functional groups of the bio-oil were analyzed by an infrared spectrum analyzer. According to relevant scholars' research, Table 4 shows the functional groups and their compounds corresponding to infrared absorption peaks of different products of biomass hydrothermal liquefaction. Figure 4 shows the infrared spectrum of water hyacinth hydrothermal liquefied bio-oil. The experimental conditions were 350°C, 20 min, 9.09 wt %, and 0.5869 g/mL.

The spectrum showed that bio-oil had a wide absorption peak at 3,520 cm^{-1}, which was the O-H stretching vibration peak of the intermolecular hydrogen bond. The

Table 3. The Organic Composition of Hydrothermal Liquefaction of Water Hyacinth (350°C, 20 min, 9.09 wt %, 0.5787 g/mL) in Oil Phase Products

S. No.	Retention time/min	Peak area ratio/%	Name	Structural formula
1	2.617	1.21	Nonane	
2	3.122	2.46	2,6-Dimethyloctane	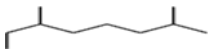
3	3.173	1.31	1-Ethyleneoxyoctane	
4	3.466	4.25	Phenol	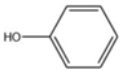
5	3.678	1.56	Decane	
6	3.857	3.13	1,2,4-Trimethylbenzene	
7	3.951	1.46	4-Methyldecane	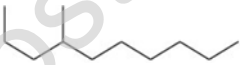
8	4.324	6.01	1-Methyl-2-pyrrolidinone	
9	4.451	1.47	2-Methyldecane	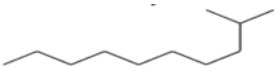
10	4.562	1.77	1-Methyl-3-isopropylbenzene	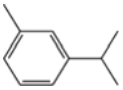
11	4.713	4.56	4-Methyl-phenol	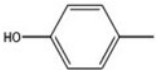
12	4.926	3.02	Undecane	
13	5.264	3.44	1-Ethyl-2-pyrrolidinone	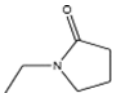
14	5.573	3.73	Naphthalene	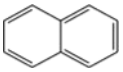
15	6.361	4.13	4-Ethylphenol	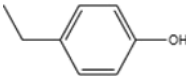
16	6.446	1.03	2-Piperidinone	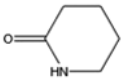
17	6.617	2.06	Dodecane	
18	6.739	1.09	1-Propyl-2-pyrrolidinone	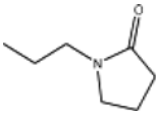
19	7.783	2.22	1-Ethyl-6-methyl-3-piperidinone	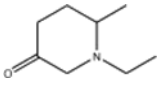

(*continued*)

TABLE 3. (CONTINUED)

S. No.	Retention time/min	Peak area ratio/%	Name	Structural formula
20	8.512	1.27	Tridecane	
21	8.863	1.37	Indole	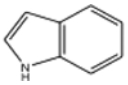
22	9.747	4.31	1-Methylpiperidine	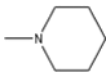
23	10.308	1.47	N-[2-hydroxyethyl]succinimide	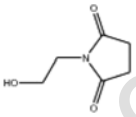
24	10.458	1.55	Tetradecane	
25	10.712	2.13	3-MethylIndole	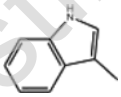
26	12.308	1.23	1-Pentadecene	
27	12.426	1.73	Pentadecane	
28	12.644	1.25	2,5-Dimethylindole	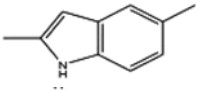
29	12.837	0.85	2,4-Bis(1,1-dimethylethyl)phenol	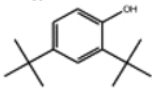
30	13.293	1.26	2-Methylhexadecane	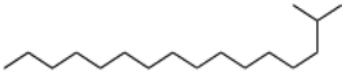
31	14.377	1.15	Hexadecane	
32	17.649	2.23	1-(2-Phenylethyl)piperidine	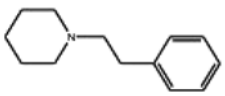
33	20.372	3.59	Pentadecanoic acid	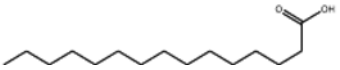
34	20.729	6.88	n-Hexadecanoic acid	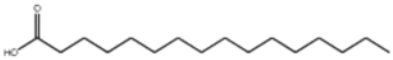
35	21.283	1.43	Dibutyl phthalate	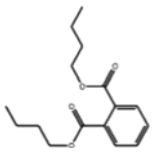
36	23.751	1.69	Octadecanoic acid	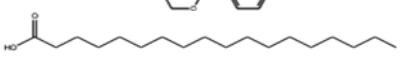
37	24.437	1.76	Hexadecanamide	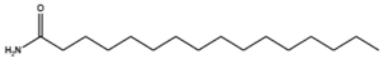

(*continued*)

TABLE 3. (CONTINUED)

S. No.	Retention time/min	Peak area ratio/%	Name	Structural formula
38	24.796	0.88	3-Octadecene-1,2-diol	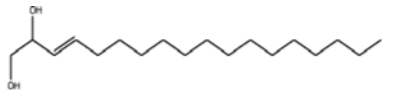
39	25.682	0.79	O-methyloxime-2-tridecanone	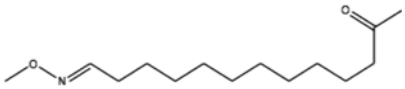
40	31.372	0.59	Heptacosane	
41	31.861	0.62	2-Ethylacridine	
42	32.764	0.52	Octacosan	

stretching vibration peaks of C-H at 3,000, 2,900, and 2,850 cm^{-1} confirmed the existence of aliphatic compounds and their derivatives in bio-oil.

Near 1,650 cm^{-1} was the vibration absorption band of C=O, which proved the presence of carboxylic acids, lipids, and ketones in the bio-oil, or the stretching vibration peak of C=C, which proved that the bio-oil contained hydrocarbons and aromatic hydrocarbons. The C-H bending vibration peak at 1,420 cm^{-1} indicated that the bio-oil contained aliphatic hydrocarbons. There were several obvious absorption peaks in the range of 1,200–1,400 cm^{-1}, which were C-O bending vibrations and C-H bending vibrations, which indicated that the bio-oil contained alcohol or phenolic compounds.

TABLE 4. FUNCTIONAL GROUPS CORRESPONDING TO INFRARED SPECTRAL ABSORPTION PEAKS AND THEIR ASSOCIATED COMPOUNDS

Wavenumber/ cm^{-1}	Function group	Attributive compound
3,600–3,050	O-H stretching vibration	Cellulose, polysaccharides
3,000–2,800	C-H stretching vibration	Fat
2,350–2,000	C ≡ C stretching vibration	Alkynes
1,750–1,640	C=O stretching vibration	Carboxylic acids, lipids, ketones
1,650–1,580	C=C stretching vibration	Aromatic, hydrocarbon
1,450–1,350	C-H bending vibration	Aliphatic hydrocarbon
1,200–1,300	C-N stretching vibration	Nitrogen-containing compound
1,300–950	C-O bending vibration	Phenol, ether, lipid
	O-H bending vibration	Alcohol
900–650	C-H bending vibration	Aromatics

The existence of phenol and phenolic alkane derivatives in bio-oil was verified by GC-MS analysis of bio-oil, which may also be a C-N stretching vibration, which confirmed the existence of nitrogen-containing compounds, such as amines, amides, and indoles. Several C-H bending vibration peaks in the range of 600–800 cm^{-1} were caused by the different number of substituents on the benzene ring and the different positions where substituents occurred, indicating that bio-oil also contained many derivatives of aromatic compounds. The results of infrared spectrum analysis of bio-oil verified the results of GC-MS analysis.

Elemental analysis. The Dulong equation is the calculation formula of the bio-oil calorific value (higher heating value [HHV]) (Channiwala and Parikh, 2002):

$$\text{HHV (MJ kg)} = 0.3383\text{C} + 1.422(\text{H-O}/8) \quad (2)$$

where C, H, and O refer to the percentage of elements in bio-oil.

Table 5 shows the analysis results of bio-oil elements obtained from water hyacinth under different hydrothermal liquefaction conditions. As shown in Table 5, the contents of C, H, and N in the bio-oil were higher than those in the raw material, while the content of O was lower. The comparison of bio-oil elements under various reaction conditions showing that the contents of H and N were not significantly different, mainly reflected in the contents of C and O. Using Dulong's formula to calculate the calorific value of bio-oil, it was found that deoxidation reaction occurred during the HTL of water hyacinth between 280°C and 350°C and the energy density increased.

The calorific value of bio-oil was the lowest and the content of O was highest at 280°C, 20 min, 9.09 wt %, and 0.5869 g/mL, which indicated that temperature was an important factor affecting the HTL of water hyacinth; the highest calorific value of bio-oil and the lowest content of O were obtained at 350°C, 60 min, 9.09 wt %, and 0.5869 g/mL, which indicated that the reaction time had an important effect on the quality of bio-oil. This result suggested that the quality of bio-oil increased with the decrease of O content.

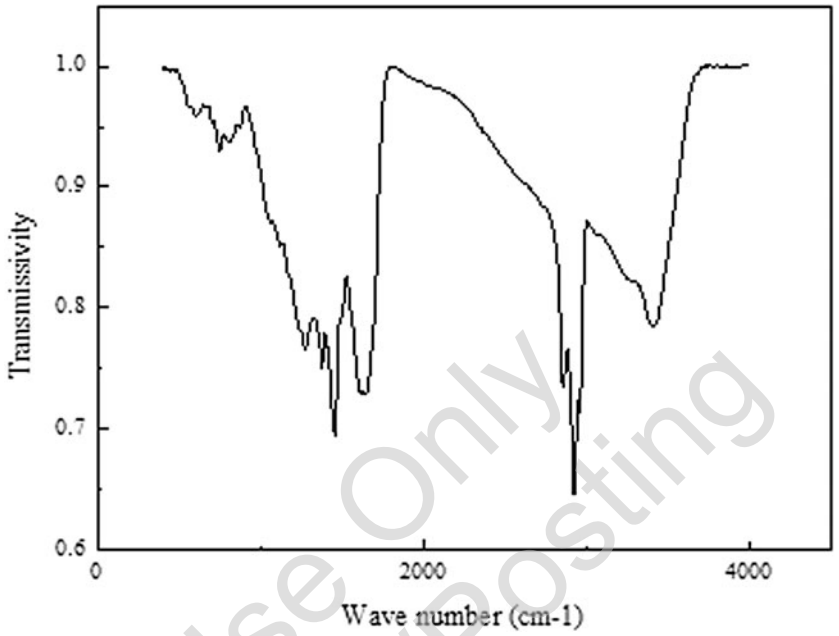

FIG. 4. Infrared spectra of oil phase products.

The energy density of bio-oil was much higher compared with raw materials, which had potential economic benefits. Additionally, the bio-oil contained 5.50–6.50% nitrogen and needed pretreatment, such as deoxidization and denitrification, before being used as fuel.

Analysis of the hydrothermal liquefaction reaction mechanism of water hyacinth

Fat. Fat is a kind of saturated higher fatty acid glyceride that is a triacylglyceride. Under high-temperature and high-pressure water, it can be rapidly hydrolyzed to form free fatty acids.

The fat of water hyacinth also contained a small amount of cholesterol, so the hydrothermally liquefied bio-oil also contained cholesterol and its derivatives (Johnson, 2012). The presence of cholesterol and its derivatives was observed in the GC-MS analysis. Due to their low content in bio-oil, there was no such organic substance in the corresponding list of GC-MS maps.

Protein. Proteins underwent a series of complex reactions during hydrothermal liquefaction and were converted into bio-oil with low nitrogen content. The reaction mechanism was the hydrolysis of C-N peptide bonds (building blocks of protein molecules) between the carboxyl and amino acids. The Maillard reaction (Fan *et al.*, 2018) occurred when amino acids were generated by protein decomposition, and monosaccharides were generated by polysaccharide hydrolysis in high-temperature and high-pressure water.

In the process of HTL, proteins in water hyacinth not only decomposed into part of the bio-oil but also reacted with reductive sugars obtained from polysaccharide hydrolysis to produce the Maillard reaction. The source of nitrogen compounds in bio-oil was the protein in water hyacinth.

Sugars. According to GC-MS and infrared spectrum analysis of water hyacinth hydrothermal liquid bio-oil, the polysaccharide contained in water hyacinth could be converted into glucose and fructose in the process of HTL.

The hydrolysis rate of sugar in water hyacinth was higher compared with protein but lower compared with crude fat. Depending on different reaction conditions, sugars may be converted into a variety of chemicals in hydrothermal reactions (Srokol *et al.*, 2004). Toor *et al.* found that sugars would be converted into benzene, propionic acid, and 4-

TABLE 5. ANALYSIS OF BIO-OIL ELEMENTS UNDER DIFFERENT HYDROTHERMAL LIQUEFACTION CONDITIONS

Reaction conditions	*C*	*H*	*N*	*O*	*HHV/(MJ/kg)*	*C/H*
280°C, 20 min, 9.09 wt %, 0.5869 g/mL	65.54	7.34	5.70	21.42	28.80	8.93
350°C, 20 min, 9.09 wt %, 0.5869 g/mL	69.69	7.44	5.50	17.34	31.07	9.37
350°C, 10 min, 9.09 wt %, 0.5869 g/mL	72.27	7.73	5.78	14.22	33.50	9.35
350°C, 40 min, 9.09 wt %, 0.5869 g/mL	74.00	7.72	5.86	12.42	33.80	9.59
350°C, 60 min, 9.09 wt %, 0.5869 g/mL	75.41	7.90	5.87	10.82	34.82	9.55
350°C, 20 min, 13.04 wt %, 0.5869 g/mL	74.32	7.81	5.60	12.27	34.07	9.52
350°C, 20 min, 23.08 wt %, 0.5869 g/mL	72.16	7.63	6.36	13.85	32.80	9.46
350°C, 20 min, 28.57 wt %, 0.5869 g/mL	71.47	7.64	6.30	14.59	32.45	9.36
350°C, 20 min, 9.09 wt %, 0.6002 g/mL	72.54	7.59	5.69	14.18	32.81	9.56
350°C, 20 min, 9.09 wt %, 0.6061 g/mL	71.15	7.24	5.72	15.89	31.54	9.83

HHV, higher heating value.

hydroxyphenyl ethanol when the temperature was above 310°C (Shuping *et al.*, 2010). In hydrothermal reactions, sugars may decompose into water-soluble organic compounds rather than nonpolar hydrocarbon structures, resulting in a lower bio-oil content in the products. Srokol *et al.* found that glucose could be decomposed into formic acid, acetic acid, lactic acid, acrylic acid, furfural, and more, under hydrothermal reaction conditions, and these polar compounds were all dissolved in water (Xiu *et al.*, 2011).

Kabyemela *et al.* mainly focused on the differential isomerization of glucose in hydrothermal reactions. They found that the decomposition rate of glucose was lower under subcritical conditions, mainly due to the weak role of differential isomerization of glucose in generating fructose, which was significantly improved under supercritical conditions (Kabyemela *et al.*, 1999). Kruse *et al.* focused on the hydrothermal reaction process of cellulose at higher temperatures. They found that the liquid phase products included glucose/fructose, furfural, phenols, carboxylic acids, aldehydes, alcohols, and more, among which phenols were the main intermediate products in the process of glucose hydrolysis (Kruse *et al.*, 2006).

These studies confirmed that the polysaccharides in water hyacinth could be converted into water-soluble organic compounds at lower temperatures in the hydrothermal liquefaction reaction.

Experimental study on SCWG of water hyacinth

The influence of reaction conditions on the SCWG characteristics of water hyacinth. Potential hydrogen production is the total amount of H_2 produced by CO through a complete water–gas conversion reaction (1) and H_2 produced by a complete reforming reaction (2) in the gas product after supercritical gasification of the material (Turn *et al.*, 1998; Minowa and Inoue, 1999; Bambang and Kim, 2008). The calculation formula of the potential hydrogen production is formula (3).

$$CO + H_2O = H_2 + CO_2 \quad (1)$$

$$CnHm + 2nH_2O \rightarrow (2n + m/2)H_2 + nCO_2 \quad (2)$$

$$HYP = (y_{H_2} + y_{CO} + 4y_{CH_4} + 5y_{C_2H_2} + 6y_{C_2H_4} + 7y_{C_2H_6}) \times 2 \quad (3)$$

Influence of reaction temperature. To investigate the effect of reaction temperature on the characteristics of water hyacinth SCWG, this article studied the reaction temperature of the water hyacinth biomass supercritical gasification process at 400–480°C. At this time, the reaction time was set as 20 min, the material concentration was 9.09%, and the change in water density ensured that the reaction pressure was 25 MPa. Figure 5 displays the influence curve of reaction temperature on the characteristics of hydrogen production of SCWG of water hyacinth. The gas yield was equal to mass of gas over initial mass of feedstock.

As shown in Fig. 5a, the gasification yield and carbon gasification yield of water hyacinth in supercritical water have the same change trend with increasing temperature. With the temperature rising from 400°C to 440°C, the gasification yield and carbon gas rate of water hyacinth slowly increased but had little change. Starting at 440°C, the increase in gasification efficiency and carbon gasification efficiency increased. The water hyacinth gasification efficiency and carbon gasification efficiency increased from 12.86% and 12.41% at 400°C to 27.02% and 28.30% at 480°C, respectively, with increases of 110.11% and 128.04%.

Some scholars have shown that when the reaction temperature is higher than 700°C, the biomass gasification efficiency can reach more than 100%, and the carbon gasification efficiency could reach more than 95%, indicating that

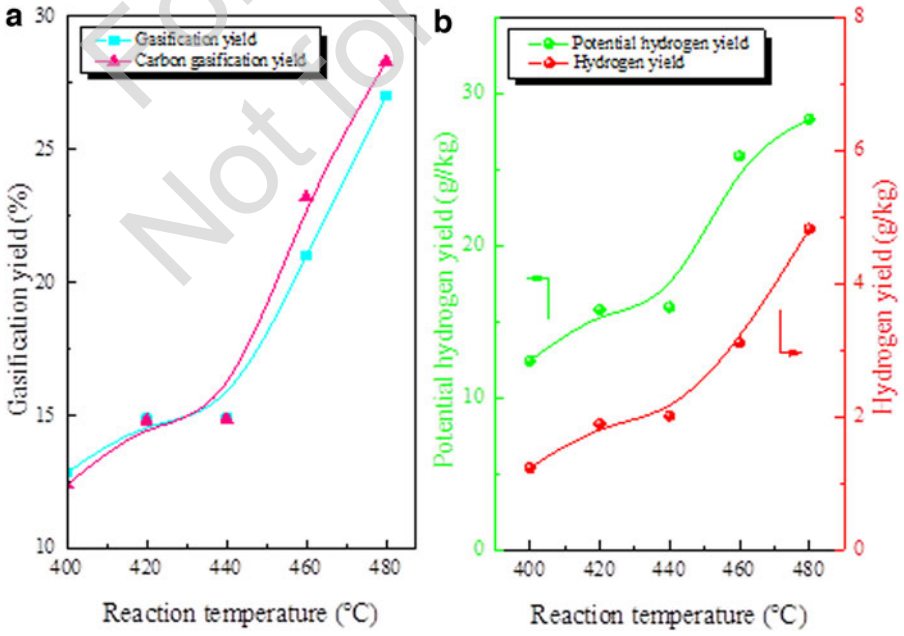

FIG. 5. Effect of reaction temperature on gas yield **(a)** and hydrogen yield **(b)** of SCWG of water hyacinth. SCWG, supercritical water gasification.

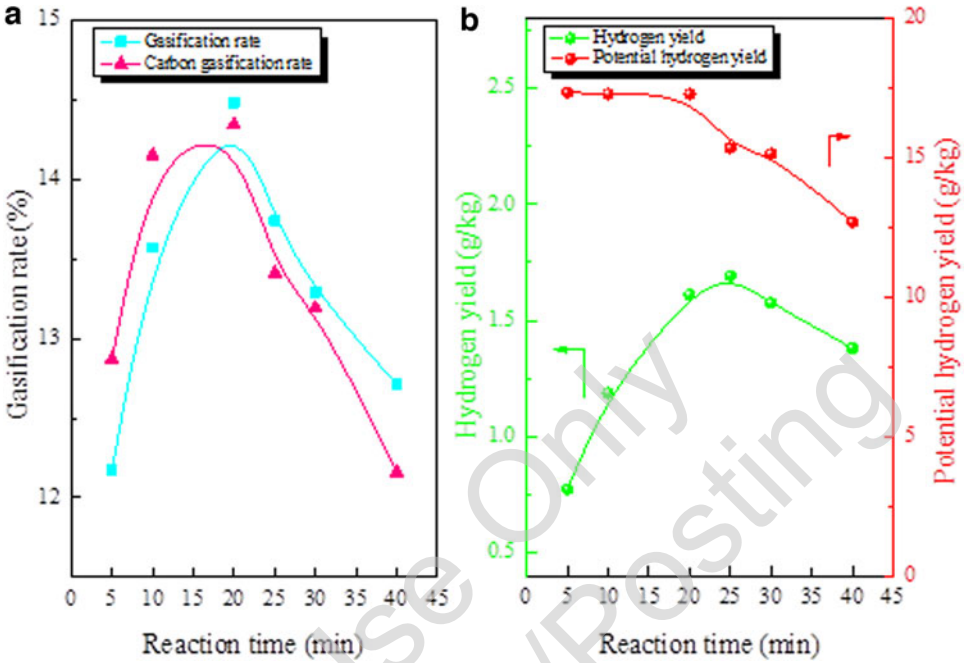

FIG. 6. Effect of reaction time on gas production rate **(a)** and hydrogen yield **(b)** of SCWG of water hyacinth.

temperature is an important factor restricting the water hyacinth supercritical gasification efficiency and carbon gasification efficiency (Ahmad *et al.*, 2016).

As Fig. 5b shows, the relationship between the potential hydrogen production and reaction temperature adopted the left principal coordinate, and the relationship between hydrogen production and reaction temperature adopted the right secondary coordinate (the same as below). As shown in the figure, hydrogen production increases with increasing temperature. The hydrogen production rate was low within the selected experimental temperature range, only 1.23% at 400°C and 4.82% at 480°C. Although absolute hydrogen production was still low, the increase was as high as 291.87%.

Some scholars point out that the hydrogen production rate is very low when the temperature is lower than 500°C, consistent with the conclusion (Turn *et al.*, 1998). The potential hydrogen production increased from 12.41% at 400°C to 28.30% at 480°C, with an increase of 128.04%. The changing trend was the same as the water hyacinth gasification efficiency.

Influence of reaction time. The reaction temperature was maintained at 420°C, the material concentration was 9.09 wt %, and the pressure was maintained at 25 MPa. Figure 6a is the curve of reaction time's influence on the gas yield and carbon gas yield of water hyacinth gasification in supercritical water. Figure 6b is the curve of reaction time's influence on the hydrogen production and potential hydrogen production of water hyacinth gasification in supercritical water.

As shown in Fig. 6a, with increasing reaction time, the gasification rate and carbon gasification of water hyacinth first increased and then decreased, showing a parabolic trend. It seems that water hyacinth first decomposed into small molecular compounds in supercritical water, and the intermediate process required a certain reaction time. When the number of activated molecules reached a certain concentration, the gasification efficiency and carbon gasification efficiency increased continuously, and the reaction time was further extended. The gasification products underwent recombination and coalescence reactions to form water-soluble organic matter or decarbonization to generate coke (Fermoso *et al.*, 2009). The reaction time was not too short and not too long, and there was an optimal reaction time.

The maximum values of gasification efficiency and carbon gasification efficiency appeared at a reaction time of 20 min, which were 14.48% and 14.34%, respectively. Compared with the minimum value of 12.17% (at 5 min) and 12.10% (at 40 min), the increased amplitude at 20 min was 19.98% and 18.51%, indicating that the degree of supercritical gasification of water hyacinth was the highest under the reaction time of 20 min.

As shown in Fig. 6b, hydrogen production first increased and then decreased with increasing reaction time, the changing trend was the same as that of the gasification rate, and hydrogen production was closely related to the gasification efficiency of water hyacinth. Hydrogen production increased from 0.77 g/kg at 5 min to 1.69 g/kg at 25 min, with an increase of 118.60%. With increasing reaction time, the potential hydrogen production decreased gradually, from 17.34 g/kg at 5 min to 12.69 g/kg at 40 min, with a decrease rate of 26.78%. In the process of supercritical gasification of water hyacinth, coke and water-soluble organic compounds were continuously generated.

Influence of feed concentration. Under a constant reaction temperature of 420°C, a reaction time of 20 min, and a reaction pressure of 25 MPa, the influence curve of the material concentration on the characteristics of SCWG of water hyacinth was studied. Figure 7 shows the influence curve of feed concentration on the gas rate and carbon gas rate of water hyacinth gasification in supercritical water and the influence curve of material concentration on the hydrogen production, and potential hydrogen production of water hyacinth gasification in supercritical water.

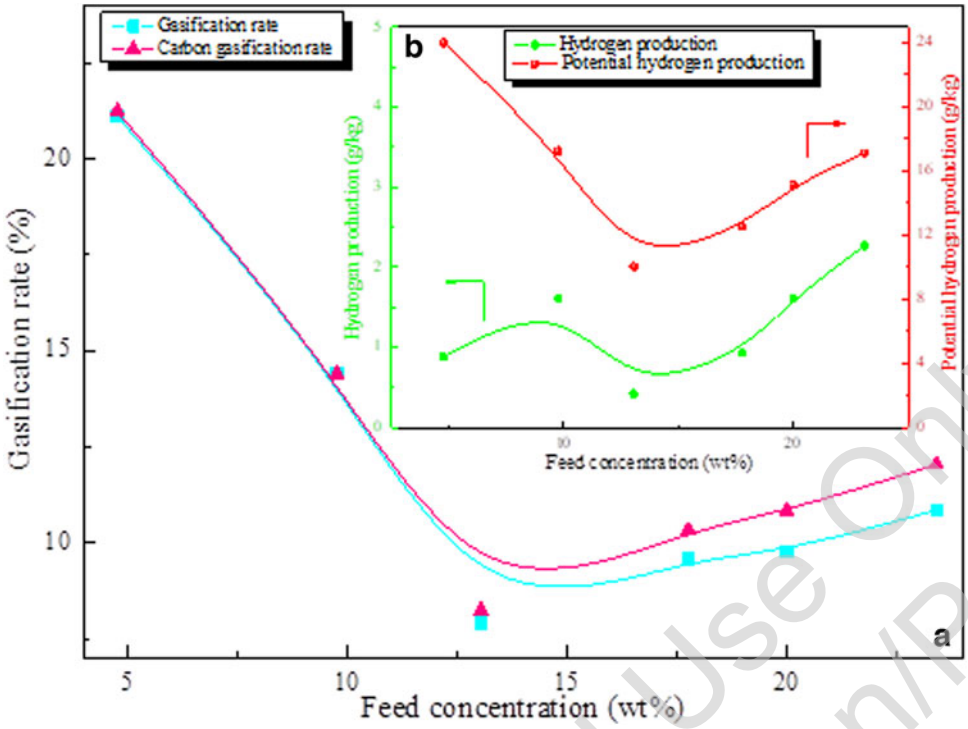

FIG. 7. Effect of feed concentration on gas production rate **(a)** and hydrogen yield **(b)** of SCWG of water hyacinth.

As shown in Fig. 7a, with increasing material concentration, the gasification rate and carbon gasification rate of water hyacinth first decreased rapidly and then increased slowly, and there was almost no difference between the gasification rate and the carbon gasification rate. Under a material concentration of 4.76 wt %, the gasification rate and carbon gasification rate of water hyacinth were 21.11% and 22.24%, respectively. Under the material concentration of 13.04 wt %, the gasification rate decreased to the minimum values of 7.90% and 8.23%, and the reduction range was 62.58% and 62.99%.

As shown in Fig. 7b, the potential hydrogen production decreased first and then increased with increasing feed concentration, which was the same as the gasification rate. The hydrogen production increased from 0.425% at 13.04 wt % to 2.265% at 23.08 wt %, with an increase of 432.94%. Combined with the changing trend of the four parameters in the two figures, it could be seen that under the feed concentration exceeding 13.04 wt %, the larger the feed concentration, the higher the hydrogen production.

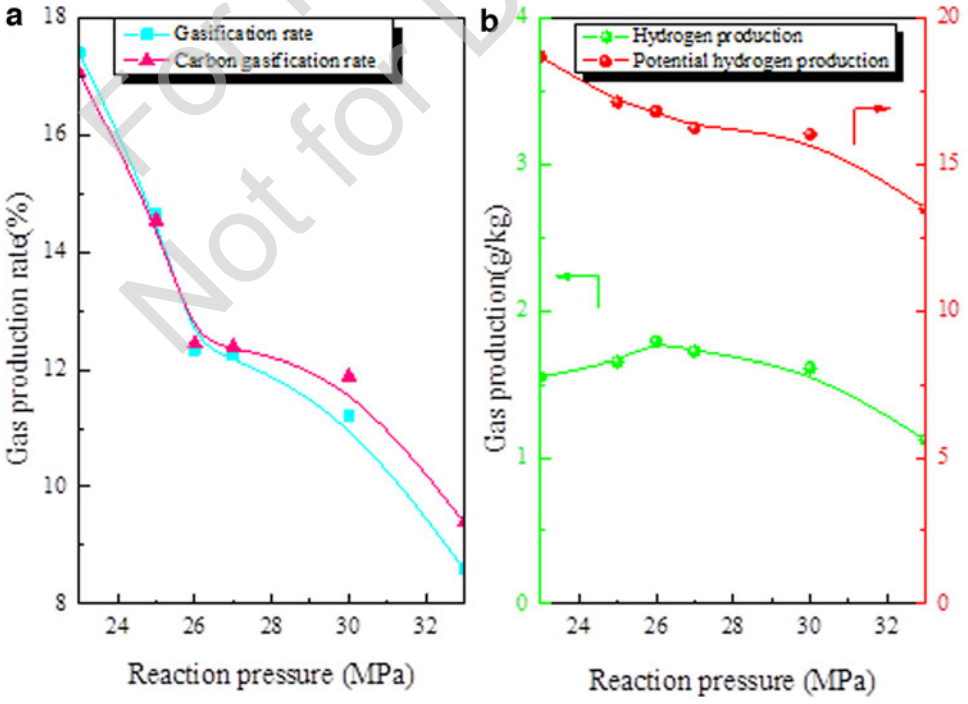

FIG. 8. Effect of reaction pressure on the gas production rate **(a)** and hydrogen yield **(b)** of SCWG of water hyacinth.

Influence of reaction pressure. In this study, the reaction temperature was 420°C, the reaction time was 20 min, and the material concentration was 9.09 wt %. The influence of different reaction pressures on the supercritical gasification effect of water hyacinth was studied. Figure 8 shows the influence curve of reaction pressure on the gas rate and carbon gas rate of water hyacinth gasification in supercritical water and the influence curve of reaction pressure on the hydrogen production and potential hydrogen production of water hyacinth gasification in supercritical water (Okolie *et al.*, 2019).

As shown in Fig. 8, with increasing pressure, the gasification rate and carbon gasification rate gradually decreased, from 17.40 and 17.04 g/kg at 23 MPa to 8.59 and 9.39 g/kg at 33 MPa, respectively, with decreasing rates of 50.63% and 44.89%. The potential hydrogen production decreased slowly with increasing pressure, from 18.66 g/kg at 23 MPa to 13.48 g/kg at 33 MPa, and the reduction range was 27.76%. Hydrogen production first increased and then decreased, reaching a maximum of 1.79 g/kg at 26 MPa. Under low reaction pressure, the gas yield was high, but the hydrogen production was low. A reaction pressure that was too high was not conducive to improving the economy of the whole system of supercritical gasification of water hyacinth. Therefore, the optimum reaction pressure was 25–27 MPa.

In conclusion, the effects of reaction temperature, reaction time, material concentration, and reaction pressure on the gasification process of water hyacinth in supercritical water were investigated. From the above analysis, the reasonable reaction conditions of supercritical gasification of water hyacinth were temperature 480°C, time 20 min, material concentration 23.08 wt %, and reaction pressure 25–27 MPa.

Analysis of gas composition

Reaction temperature. Figure 9 shows the trend of the reaction temperature on the gas composition of water hyacinth gasification in supercritical water. The reaction time was 20 min, the feed concentration was 9.09 wt %, and the reaction pressure was 25 MPa, which remained unchanged.

As shown in Fig. 9, the CO_2 content was the highest among all gases. With increasing temperature, the volume percentage of CO_2 gradually decreased from 50.83% at 400°C to 35.80% at 480°C, with a decrease of 25.97%. The CO_2 content decreased, the total combustible gas content increased, and each component gas's variation trend was different. The CO and C_2H_4 contents were maintained at a low level, not exceeding 5%, and the CO content rose to 12.17% suddenly at 480°C. The percentage of H_2 increased from 15.91% at 400°C to 28.59% at 480°C, with an increase of 79.70%. The percentage of CH_4 decreased from 32.61% at 400°C to 24.99% at 480°C, with a decrease rate of 23.37%.

At temperatures below 400°C, the combustible gas composition of biomass gasified in supercritical water was mainly CH_4, with less H_2 content, consistent with the conclusion (Patel *et al.*, 1993).

Reaction time. Figure 10 shows the trend chart of the gas composition change of reaction time on water hyacinth gasification in supercritical water. The reaction temperature was maintained at 420°C, the material concentration was 9.09 wt %, and the reaction pressure was maintained at 25 MPa. As shown in the figure, the CO_2 content was ~50% and increased slowly with increasing reaction time. The CH_4 content decreased from 45.10% when the reaction time was 5 min to 22.76% at a reaction time of 40 min, with a decrease rate of 49.53%. The H_2 content first increased and then decreased slightly and reached a maximum value of 20.63% at a reaction time of 25 min. During all reaction times, both the CO and C_2H_4 contents were below 4%.

Feed concentration. Under a reaction temperature of 420°C, a reaction time of 20 min, and a reaction pressure of 25 MPa, the variation trend of the gas composition of water hyacinth gasification under supercritical water under the influence of the material concentration was studied, as shown in Fig. 11.

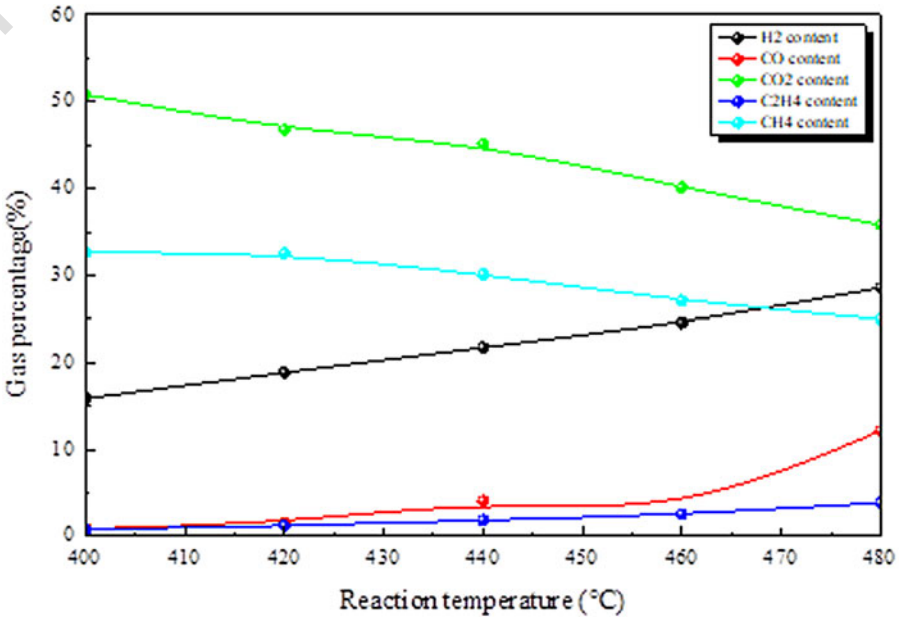

FIG. 9. Effect of reaction temperature on gas composition in SCWG of water hyacinth.

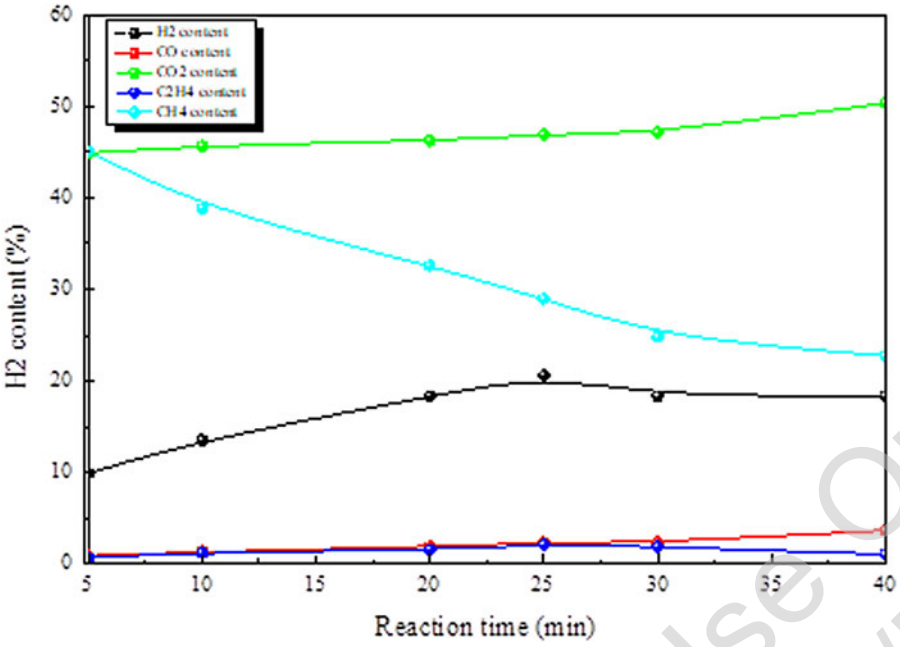

FIG. 10. Effect of reaction time on gas composition in SCWG of water hyacinth.

With increasing feed concentration, the CO_2 content decreased from 54.24% under the material concentration of 4.76 wt % to 28.89% under the material concentration of 23.08 wt %, with a decrease rate as high as 46.74%. With increasing material concentration, the CH_4 content increased slowly and was maintained at a high level, increasing by 42.15%. The maximum H_2 content reached 32.41% when the material concentration was 23.08 wt %, which increased by nearly 4 times compared with the minimum. The contents of CO and C_2H_4 were maintained at a low level within the selected feed concentration range. With increasing material concentration, the content of CO_2 in the gas decreased continuously, while the content of H_2 and CH_4 with high combustion value increased.

Therefore, the increase in material concentration was conducive to an improvement of the produced gas quality.

Reaction pressure. The reaction temperature, reaction time, and material concentration were kept unchanged at 420°C, 20 min, and 9.09 wt %. The influence of reaction pressure on the gas composition of water hyacinth gasification in supercritical water is shown in Fig. 12. With increasing reaction pressure, the CO_2 content gradually decreased, from 50.94% at 23 MPa to 38.17% at 33 MPa,

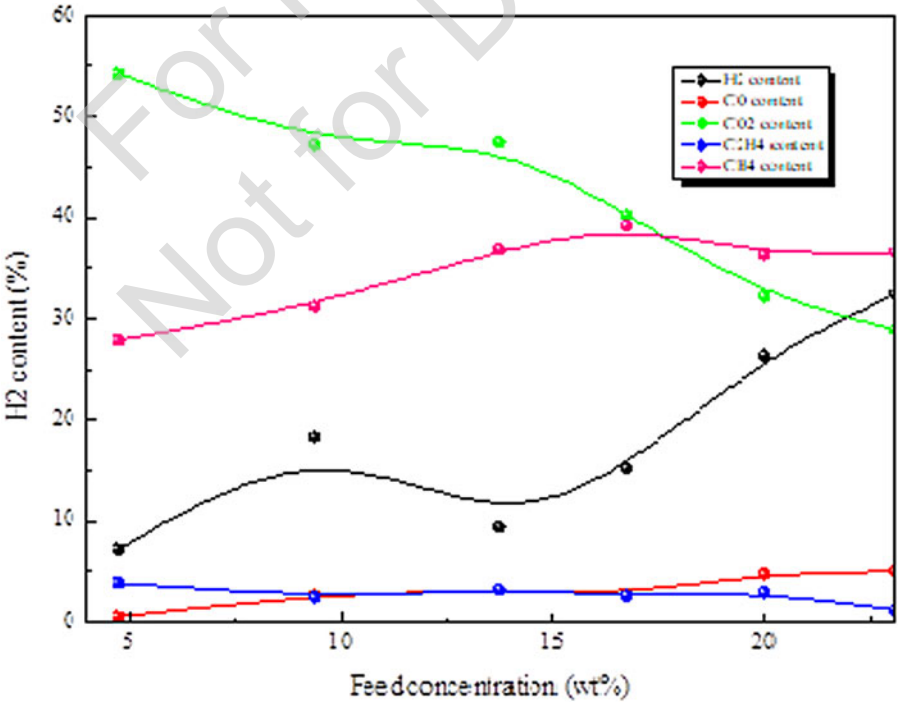

FIG. 11. Effect of feed concentration on gas composition in SCWG of water hyacinth.

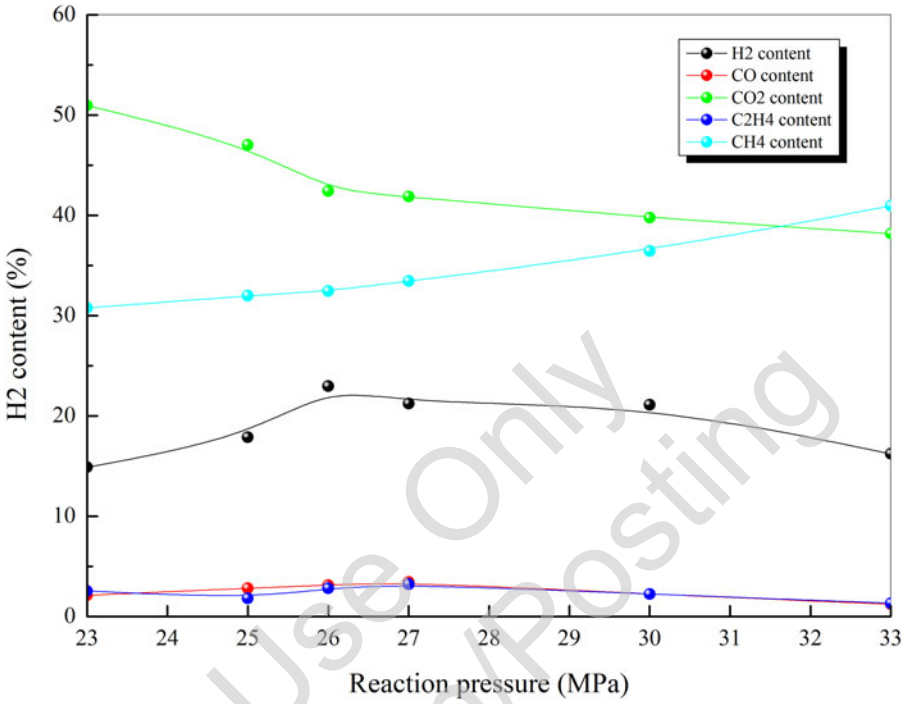

FIG. 12. Effect of reaction pressure on gas composition in SCWG of water hyacinth.

with a decrease rate of 25.07%. With increasing reaction pressure, the CH_4 content increased from 30.76% at 23 MPa to 40.95% at 33 MPa, with an increase of 33.13%. The H_2 content rose first and then dropped slowly and reached its maximum value at 26 MPa, which was 22.95%. The contents of CO and C_2H_4 were maintained at a low level within the selected material concentration range.

The results showed that the contents of CO, C_2H_2, C_2H_4, and C_2H_6 were very low and had little change. The content of CO_2 was the highest of all gas components. Although the content increased with increasing reaction time, it decreased with increasing reaction temperature, material concentration, and reaction pressure. The CH_4 content decreased with increasing reaction temperature and reaction time but increased with increasing material concentration and reaction pressure. The content of H_2 increased with increasing reaction temperature and concentration. With increasing reaction time and increasing reaction pressure, the content of H_2 first increased and then decreased slowly.

Conservation analysis of carbon during SCWG of water hyacinth. After water hyacinth was gasified in supercritical water, part of the carbon was transferred to the gas, which was characterized by the carbon gasification rate. It was mentioned earlier in the article that the influence of each reaction condition on the carbon gasification rate was analyzed. Some C elements were transferred to organic and inorganic substances that were soluble in water and dissolved in water. A TOC analyzer was used to measure the TC in the aqueous phase products, calculate the carbon content in the aqueous phase, and characterize the content with the carbon migration rate (He *et al.*, 2014). In this section, the conservation analysis of carbon was mainly carried out by calculating the carbon gas rate and carbon migration rate. The data records are shown in Table 6.

In this study, the experimental method of a single impact factor was adopted. The other reaction conditions for the reaction temperature were 20 min, 9.09 wt %, and 25 MPa; the other reaction conditions for the reaction time were 420°C, 9.09 wt %, and 25 MPa; the other reaction conditions

TABLE 6. MIGRATION AND TRANSFORMATION OF CARBON UNDER DIFFERENT REACTION CONDITIONS

Reaction conditions	*Carbon gasification rate/%*	*Carbon migration rate/%*	*Summation/ %*
400°C	12.41	79.46	91.87
420°C	14.34	76.83	91.17
440°C	14.54	75.37	89.91
460°C	22.68	70.16	92.84
480°C	28.30	62.48	90.78
5 min	12.94	79.61	92.55
10 min	14.03	77.89	91.92
20 min	14.34	76.83	91.17
25 min	13.37	78.83	92.20
30 min	13.06	78.35	91.41
40 min	12.10	81.42	93.52
4.76 wt %	22.24	69.24	91.48
9.09 wt %	14.34	76.83	91.17
13.04 wt %	8.23	82.36	90.59
16.67 wt %	9.41	80.87	90.28
20 wt %	10.12	79.14	89.26
23.08 wt %	11.42	77.86	89.28
23 MPa	17.04	74.13	91.17
25 MPa	14.34	76.83	91.17
26 MPa	12.68	79.41	92.09
27 MPa	12.57	80.76	93.33
30 MPa	11.80	78.48	90.28
33 MPa	9.39	83.53	92.92

for the material concentration were 420°C, 20 min, and 25 MPa; and the other reaction conditions for the reaction pressure were 420°C, 20 min, and 9.09 wt %.

It was mentioned before that with increasing temperature, the carbon gas yield of water hyacinth first slowly rose and then rapidly increased, with an increase of 128.04%. The carbon gas yield first increased and then decreased with the extension of reaction time; it first rapidly decreased and then slowly increased with the increase of material concentration; it continued to decrease with the increase of pressure, and all change trends were not the same.

A TOC analyzer was used to measure the TC in the aqueous phase and determine carbon mobility in the aqueous phase. In addition, during the gasification of water hyacinth in supercritical water, a part of carbon was transformed into coke and existed in the solid residue (Zhao *et al.*, 2012). Literature research found that the content of coke was very small, so it was not measured and analyzed. If the neglected part of the carbon was included to the sum, the carbon balance would probably be improved in the supercritical gasification process of water hyacinth.

In terms of HHV, the HHV of bio-oil generated under HTL conditions of 50°C, 60 min, 9.09 wt %, and 0.5869 g/mL was the highest, which was 34.82 MJ/kg. The calorific value of SCWG could be replaced by the calorific value of hydrogen yield and potential hydrogen yield calculated. The HHV was the sum of hydrogen yield and potential hydrogen yield timed the hydrogen HHV. In Fig. 5, the highest calorific value could be calculated simply as 4.64 MJ/kg at 480°C.

Conclusion

The conditions showing the highest bio-oil yield for HTL of water hyacinth were 350°C, 50 min, 20 wt % of feed concentration, and 0.6002 g/mL of water density. As the reaction temperature increased, the carbon recovery rate in the aqueous phase decreased, which decreased significantly in the low-temperature zone and slowly in the high-temperature zone. The carbon recovery rate in the aqueous phase also decreased with the prolongation of reaction time and the increase of material concentration. The water density had little effect on the mobility of aqueous phase C. The increase of reaction temperature promoted the hydrolysis of protein in water hyacinth into water-soluble substances and the increase of recovery rate of aqueous phase N, and the reaction temperature was the most important influencing factor.

As the material concentration increased, the N recovery rate in the aqueous phase continued to decrease, and the nitrogen was transferred to the oil phase. The recovery rate of aqueous phase N increased slightly with increasing reaction time. The calorific value of bio-oil was much higher compared with water hyacinth raw material. In the HTL, the fat was hydrolyzed into fatty acids, decarboxylation of fatty acids formed aliphatic hydrocarbons, protein not only hydrolyzed the C-N peptide bond but also reacted with aldose to form ketones and nitrogen-containing compounds, and the hydrolysis and cyclization of polysaccharides produced phenols.

The conditions showing the highest gas yield of SCWG of water hyacinth were 480°C, 20 min, 23.08 wt %, and 25–27 MPa. CO_2 had the highest content among all gas components, and the content increased with increasing reaction time and decreased with increasing reaction temperature, feed concentration, and reaction pressure. The content of CH_4 decreased with increasing reaction temperature and reaction time and increased with increasing material concentration and reaction pressure. The content of H_2 increased with increasing reaction temperature, increased with reaction time too (up to 25 min), and also increased with increasing feed concentration. The mass of carbon in the process of supercritical gasification of water hyacinth was conserved.

The energy conversion efficiency of SCWG of water hyacinth in this experiment is far lower compared with HTL. However, SCWG still has a large development space in terms of reaction temperature and material concentration. In contrast, HTL has great advantages in investment cost and equipment safety.

Author Disclosure Statement

No competing financial interests exist.

Funding Information

This study was funded by Guangxi Natural Science Foundation of China.

References

Ahmad, A.A., Zawawi, N.A., Kasim, F.H., Inayat, A., and Khasri, A. (2016). Assessing the gasification performance of biomass: A review on biomass gasification process conditions, optimization and economic evaluation. *Renew. Sust. Energ. Rev.* 53, 1333.

Amrullah, A., and Matsumura, Y. (2017). Supercritical water gasification of sewage sludge in continuous reactor. *Bioresour. Technol.* 249, 276.

Bambang, V., and Kim, J. (2008). Hydrogen production by gasification of isooctane using supercritical water. *Int. J. Green Energy* 5, 322.

Bo, Z., Zhixia, H., Haitao, C., Sabariswaran, K., Zhixiang, X., and Xun, H. (2018). Effect of acidic, neutral and alkaline conditions on product distribution and biocrude oil chemistry from hydrothermal liquefaction of microalgae. *Bioresour. Technol.* 270, 129.

Channiwala, S.A., and Parikh, P.P. (2002). A unified correlation for estimating HHV of solid, liquid and gaseous fuels. *Fuel* 81, 1051.

Demirbaş, A. (1998). Yields of oil products from thermochemical biomass conversion processes. *Energy Convers. Manag.* 39, 685.

Dimitriadis, A., and Bezergianni, S. (2017). Hydrothermal liquefaction of various biomass and waste feedstocks for biocrude production: A state of the art review. *Renew. Sust. Energ. Rev.* 68, 113.

Duan, P., and Savage, P.E. (2010). Hydrothermal liquefaction of a microalga with heterogeneous catalysts. *Ind. Eng. Chem. Res.* 50, 52.

Duan, P.G., Yang, S.K., Xu, Y.P., Wang, F., Zhao, D., and Weng, Y.J. (2018). Integration of hydrothermal liquefaction and supercritical water gasification for improvement of energy recovery from algal biomass. *Energy* 155, 734.

Elliott, D.C., Biller, P., Ross, A.B., Schmidt, A.J., and Jones, S.B. (2015). Hydrothermal liquefaction of biomass: Developments from batch to continuous process. *Bioresour. Technol.* 178, 147.

Faeth, J.L., Valdez, P.J., and Savage, P.E. (2013). Fast hydrothermal liquefaction of nannochloropsis sp. to produce biocrude. *Energy Fuels* 27, 1391.

Fan, Y., Hornung, U., Dahmen, N., and Kruse, A. (2018). Hydrothermal liquefaction of protein-containing biomass: Study of model compounds for Maillard reactions. *Biomass Convers. Biorefin.* 8, 909.

Fermoso, J., Arias, B., Plaza, M.G., Pevida, C., Rubiera, F., Pisa, J.J., García-Pea, F., and Casero, P. (2009). High-pressure co-gasification of coal with biomass and petroleum coke. *Fuel Process. Technol.* 90, 926.

He, H., Shan, J., and Zhang, X. (2014). Analysis of total organic carbon in soil by TOC analyzer. In *Analytical Instrumentation*. p. 59.

Johnson, M.C. (2012). Hydrothermal processing of high-lipid biomass to fuels. Massachusetts Institute of Technology.

Kabyemela, B.M., Adschiri, T., Malaluan, R.M., and Arai, K. (1999). Glucose and fructose decomposition in subcritical and supercritical water:? Detailed reaction pathway, mechanisms, and kinetics. *Ind. Eng. Chem. Res.* 38, 2888.

Kruse, A., and Gawlik, A. (2003). Biomass conversion in water at 330–410°C and 30–50 MPa: Identification of key compounds for indicating different chemical reaction pathways. *Ind. Eng. Chem. Res.* 42, 267.

Kruse, A., Maniam, P., and Spieler, F. (2006). Influence of proteins on the hydrothermal gasification and liquefaction of biomass. 2. Model compounds. *Ind. Eng. Chem. Res.* 46, 87.

Kunaver, M., Jasiukaitytė, E., Čuk, N., and Guthrie, J.T. (2010). Liquefaction of wood, synthesis and characterization of liquefied wood polyester derivatives. *J. Appl. Polym. Sci.* 115, 1265.

Minowa, T., and Inoue, S. (1999). Hydrogen production from biomass by catalytic gasification in hot compressed water. *Renew. Energy* 16, 1114.

Mishima, D., Kuniki, M., Sei, K., Soda, S., Ike, M., and Fujita, M. (2008). Ethanol production from candidate energy crops: Water hyacinth (*Eichhornia crassipes*) and water lettuce (*Pistia stratiotes* L.). *Bioresour. Technol.* 99, 2495.

Nanda, S., Reddy, S.N., Vo, D.N., Sahoo, B.N., and Kozinski, J.A. (2018). Catalytic gasification of wheat straw in hot compressed (subcritical and supercritical) water for hydrogen production. *Energy Sci. Eng.* 6, 448.

Okolie, J.A., Rana, R., Nanda, S., Dalai, A.K., and Kozinski, J.A. (2019). Supercritical water gasification of biomass: A state-of-the-art review of process parameters, reaction mechanisms and catalysis. *Sustain. Energy Fuels* 3, 578.

Patel, V., Desai, M., and Madamwar, D. (1993). Thermochemical pretreatment of water hyacinth for improved biomethanation. *Appl. Biochem. Biotechnol.* 42, 67.

Peterson, A.A., Vogel, F, Lachance, R.P., Fröling, M., and Tester, J.W. (2008). Thermochemical biofuel production in hydrothermal media: A review of sub- and supercritical water technologies. *Energy Environ. Sci.* 1, 32.

Reddy, S.N., Nanda, S., Dalai, A.K., and Kozinski, J.A. (2014). Supercritical water gasification of biomass for hydrogen production. *Int. J. Hydrogen Energy* 39, 6912.

Rodriguez Correa, C., and Kruse, A. (2017). Supercritical water gasification of biomass for hydrogen production—Review. *J. Supercrit. Fluids* 133, 573.

Shakya, R., Adhikari, S., Mahadevan, R., Hassan, E.B., and Dempster, T.A. (2017). Catalytic upgrading of bio-oil produced from hydrothermal liquefaction of Nannochloropsis sp. *Bioresour. Technol.* 252, 28.

Shuping, Z., Yulong, W., Mingde, Y., Kaleem, I., Chun, L., and Tong, J. (2010). Production and characterization of bio-oil from hydrothermal liquefaction of microalgae Dunaliella tertiolecta cake. *Energy* 35, 5406.

Srokol, Z., Bouche, A.G., Estrik, A.V., Strik, R.C.J., Maschmeyer, T., and Peters, J.A. (2004). Hydrothermal upgrading of biomass to biofuel; studies on some monosaccharide model compounds. *Carbohydr. Res.* 339, 1717.

Toor, S.S., Rosendahl, L.A., Hoffmann, J., Pedersen, T.H., and Søgaard, E.G. (2011). Hydrothermal liquefaction of biomass: A review of subcritical water technologies. *Energy* 36, 2328.

Turn, S., Kinoshita, C., and Zhang, Z. (1998). An experimental investigation of hydrogen production from biomass gasification. *Int. J. Hydrogen Energy* 23, 641.

Uddin, M.N., Daud, W.M.A.W., and Abbas, H.F. (2014). Effects of pyrolysis parameters on hydrogen formations from biomass: A review. *Cheminform* 45, 10467.

Valdez, P.J., Nelson, M.C., Wang, H.Y., Lin, X.N., and Sauage, P.E. (2012). Hydrothermal liquefaction of Nannochloropsis sp.: Systematic study of process variables and analysis of the product fractions. *Biomass Bioenergy* 46, 317.

Xiu, S., Shahbazi, A., Shirley, V.B., and Wang, L. (2011). Swine manure/Crude glycerol co-liquefaction: Physical properties and chemical analysis of bio-oil product. *Bioresour. Technol.* 102, 1928.

Yeh, T.M., Dickinson, J.G., Franck, A., Linic, S., Thompson, L.T., and Savage, P.E. (2012). Hydrothermal catalytic production of fuels and chemicals from aquatic biomass. *J. Chem. Technol. Biotechnol.* 88, 13.

Zhao, L., Zhang, J., Sheng, C.D., Wang, K., and Ding, Q.Z. (2012). Dissolution characteristics of inorganic elements existing in biomass during the supercritical water gasification process. *Energy Sources* 34, 1893.